scientific reports

Check for updates

OPEN

Comparison of the establishment of a rabbit model of carpal tunnel syndrome under ultrasound-guided and landmark-guided methods

Qiao-Yin Zhou[1,2], Tian-Hua Li[1,2], Jing-Yuan Zeng[1,2], Dan-Tong Wu[1,2], Yun-Nan Li[1,2], Qian Chen[3] & Shi-Liang Li[1,2]✉

A simple and feasible rabbit model of carpal tunnel syndrome (CTS) was established using an animal experimental study. Twenty-four New Zealand white rabbits were randomized into a normal group (Group C), a glucose injection model group (Groups N-M) and an ultrasound-guided injection model group (Groups U-M). Each group consisted of 8 rabbits.Electrophysiological and ultrasound examinations were performed before sampling. Hematoxylin-eosin (H&E) staining and electron microscopy were performed to observe the neuropathological changes. During electrophysiological testing 1 week after modeling, the amplitudes of the sensory nerve conduction velocity (SNCV), distal motor latency (DML) and compound muscle action potential (CMAP) in the U-M group were significantly different compared to the C group and the N-M group ($P < 0.05$). Five weeks after modeling, the amplitudes of the SNCV, DML and CMAP in the U-M group and the C group were significantly different ($P < 0.05$). These differences were statistically significant compared to the DML and CMAP in the N-M group ($P < 0.05$), and the changes in these parameters were more significant than the results 1 week after modeling ($P < 0.05$). The difference in CMAP amplitude between the N-M group and C group was statistically significant ($P < 0.05$), but the other parameters were not significantly different ($P > 0.05$). Compared to the original modeling method, four injections of 0.3 ml of 10% glucose solution under ultrasound guidance reduced the time required to establish the disease model and increased the stability of the model. Therefore, this technique is a simple and feasible method for establishing a model of rabbit carpal tunnel syndrome.

Keywords Ultrasound guidance, Needle knife, Carpal tunnel syndrome

Carpal tunnel syndrome (CTS) is a neuropathy caused by compression of the median nerve as it passes through the carpal tunnel at the wrist. It is the most common nerve compression lesion, accounting for 90% of all neuropathies[1]. A variety of animal models of carpal tunnel syndrome have been established to investigate the pathogenesis of carpal tunnel syndrome and the efficacy of treatment methods. However, most of these models are pathological models, and few models fully replicate the natural process of the disease. Among these methods, the glucose solution injection method is the simplest and easiest to perform. This modeling method is reproducible, has a high success rate and is suitable for large-scale animal experiments. It may be used to study the effect and mechanism of fibrosis on nerves and evaluate the curative effect of treatment methods.

However, this modeling method involved making a small incision near the proximal end of the carpal tunnel and injecting 0.1 ml of 10% glucose solution into the synovial membrane surrounding the superficial flexor tendon of the middle finger, which increased the technical difficulty and the risk of surgical infection. Due to the advantages of portability, lack of radiation, low cost, and high accuracy, ultrasound has become increasingly popular in joint cavity injection applications[2]. Similar animal studies confirmed that ultrasound guidance improved the accuracy of joint injection in animal models, such as rabbits and rats[3–6]. Therefore, the present study optimized the injection route into the carpal tunnel of rabbits using ultrasound guidance. We compared the functional and morphological changes in the median nerve after modeling and examined the feasibility

[1]College of Traditional Chinese Medicine, Fujian University of Traditional Chinese Medicine, Fujian 350108, Fuzhou, China. [2]Key Laboratory of Orthopedics & Traumatology of Traditional, Chinese Medicine and Rehabilitation (FuJian university of TCM), Ministry of Education, Fujian 350108, Fuzhou, China. [3]The Third Affiliated Hospital of Fujian University of Traditional Chinese Medicine, Fujian 350108, Fuzhou, China. ✉email: 19505953185@163.com

and stability of the improved modeling method to provide experimental evidence for establishing a simple and feasible rabbit carpal tunnel syndrome model.

Materials and methods

Experimental animals

Healthy male New Zealand rabbits (weighing 2.5–3.5 kg, 6 months old) were provided by the animal experiment center (license number: syxk (min) 2019-0007). The humidity of the breeding environment was approximately 75%, the temperature was 22 ± 2 °C, and the light: dark cycle was 12 h:12 h. The animals had free access to water and food and were allowed to move freely in their cages (approximately 65 cm×45 cm×30 cm). Surgery was performed in strict accordance with the guidelines for experimental animal research of Fujian University of Traditional Chinese Medicine and was approved by the Animal Experiment Ethics Committee (No. FJTCMIACUC2021077). All animal operation and procedures were conducted according to the approved guidelines and were in accordance with ARRIVE's guidelines.

Experimental grouping

Healthy male New Zealand rabbits were divided into three groups using the random number table method, with 8 rabbits in each group.

The normal group (Group C) received no treatment.

In the glucose injection model group (Group N-M), the bilateral forepaws of New Zealand rabbits were modeled using glucose injection.

In the ultrasound-guided injection model group (Group U-M), bilateral forepaws were modeled via ultrasound-guided glucose injection.

Four rabbits were euthanized from each group at 1 week and 5 weeks after modeling.

Experimental modeling

(1) Glucose injection method: Urethane (4 ml/kg, 20%) was administered via the ear marginal vein, and the muscles of New Zealand rabbits were well relaxed. There was no spontaneous activity in the clamp. After the corneal reflex was blunted, the rabbits were fixed in the supine position on the operating table. The hair in the wrist area of the animal's forepaw was removed using an electric shaver and hair removal cream, and the skin was cleaned and disinfected. Rabbit's wrist tunnels can be located by body surface identification. Determine the proximal boundary of the wrist tunnel through the wrist bone. Determine the remote boundary of the denomination of the vectors through the triangular cartilage. This triangle cartilage is a unique structure of the rabbit's front paw.

A 3-4-mm incision was made 1 cm proximal to the carpal tunnel of the forepaw. The flexor tendon was identified by moving the middle finger of the forepaw. A 5.5% intravenous infusion needle was inserted along the surface of the superficial flexor tendon of the middle finger to ensure that 0.1 ml of the 10% glucose solution was injected into the synovium between the tendon and the transverse carpal ligament (TCL) (Fig. 1). The position of the needle tip was confirmed via placement of a needle of the same size on the skin surface. The wound was sutured with 5 – 0 Vicryl suture. The treatments were administered once weekly, 4 times in total.

(2) Ultrasound-guided glucose injection method: After anesthesia and shaving using the method described above, the short axis of the LH15-6 linear array frequency conversion probe was placed on the wrist joint of the forepaw. After the ultrasound showed the carpal tunnel image, the median nerve was located. A 1-ml syringe was used to create an out-of-plane needle at the proximal boundary of the carpal tunnel, and 0.3 ml of a 10% glucose solution was injected around the median nFig. (Fig. 2). The treatments were administered once weekly, 4 times in total.

Experimental indicators

(1) Electrophysiological examination: New Zealand rabbits were shaved after anesthesia using the same method. The recording electrode was located in the thenar muscle of the forepaw, and the stimulating electrode was located 2–3 cm from the recording pFig. (Fig. 3). The stimulation was repeated three times at an interval of 30 s, and the average value was used. All rabbits underwent electrophysiological examination of bilateral forepaws, and the amplitudes of the sensory nerve conduction velocity (SNCV), distal motor latency (DML) and compound muscle action potential (CMAP)were measured before the materials were collected.
(2) Ultrasonic imaging examination: After anesthesia and shaving, the bilateral forepaws of the rabbits were examined via ultrasound. The long axis of the LH15-6 linear array frequency conversion probe was placed in the wrist region, and the diameter of the median nerve and TCL thickness were measured before sampling. The mechanical properties of carpal tunnel tissue were qualitatively evaluated using ultrasonic stress elastography.
(3) Hematoxylin-eosin (H&E) staining: At the end of the experiment, the animals were sacrificed via air injection through the ear vein, and the left forepaw carpal tunnel was quickly removed. The triangular cartilage of the transverse carpal ligament of the rabbit was used as the carpal tunnel boundary marker. After removal of the carpal bone, the carpal tunnel soft tissue was fixed in 4% paraformaldehyde for 48 h. The fixed specimen was removed and rinsed with running water for 12 h before block trimming. The tissues were dehydrated in a gradient of 70%, 80%, 90%, 95%, and 100% ethanol, cleared with xylene, waxed, embedded,

Fig. 1. Schematic diagram of glucose injection.

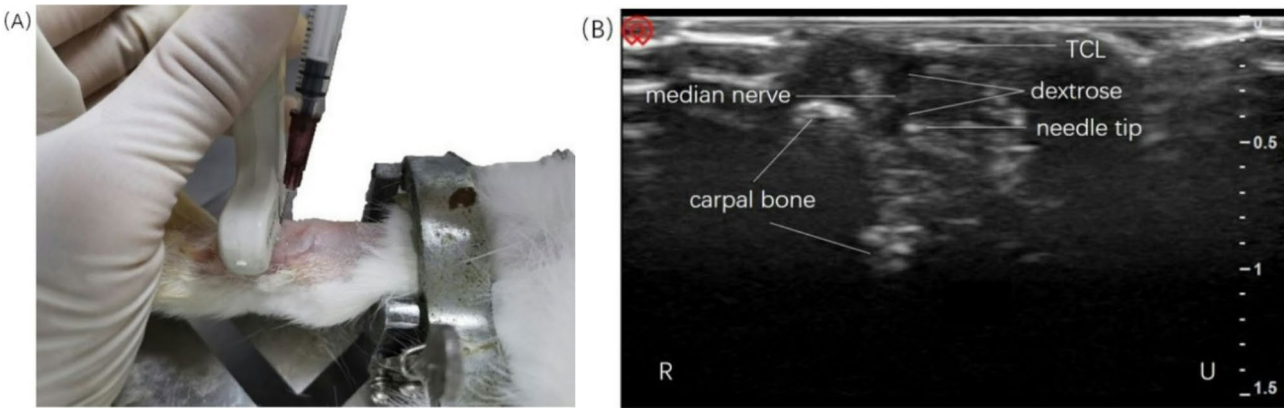

Fig. 2. Ultrasound guided glucose injection. Schematic diagram of ultrasound guided glucose injection (B) Probe cross section scanning diagram. Radial (label "R"); Ulnar (label"U").

sectioned, baked, and stained to observe pathological changes in the median nerve, transverse carpal ligament, and subsynovial connective tissue (SSCT) in the carpal tunnel.

(4) Transmission electron microscopy: A 5-mm piece of median nerve from the right forepaw carpal tunnel of rabbits was placed in a 2.5% glutaraldehyde solution for 24 h, trimmed to approximately 1 mm^3, and rinsed with a 0.1 M phosphate rinsing solution 3 times for 15 min each. The sample was placed in a 1% osmium acid solution at 4 °C for 2 h, then placed in ethanol for gradient dehydration and soaked for embedding. The

Fig. 3. Schematic diagram of electrophysiological detection.

embedding plate was placed in a 60 °C oven for 48 h. After the resin was fully polymerized, the embedded block was removed for use. After the block was roughed, an ultrathin sectioning machine was used to create ultrathin sections at the desired location. The sections were stained with a uranium acetate saturated alcohol solution and lead citrate solution. The morphology of the nerve fibers and Schwann cells was observed under a transmission electron microscope, and images were acquired.

Group	Number of cases	SNCV(m/s)	DML(ms)	CMAP amplitude(mv)
C	4	87.76 ± 6.16	1.40 ± 0.14	7.49 ± 0.96
N-M	4	76.96 ± 8.61	1.42 ± 0.16	7.36 ± 0.75
U-M	4	65.18 ± 2.82*△	1.72 ± 0.09*△	4.39 ± 1.28*△
P		0.000	0.000	0.000

Table 1. Electrophysiological examination results of each group 1 week after modeling($\bar{x} \pm s$). OMST: Olmesartan. *P<0.05 vs. normal group, △P<0.05 vs. glucose injection model group.

Group	Number of cases		SNCV(m/s)	DML(ms)	CMAP amplitude(mv)
C		4	89.25 ± 6.36	1.53 ± 0.12	7.72 ± 0.83
N-M		4	69.48 ± 3.83	1.58 ± 0.14	4.17 ± 0.98*
U-M		4	58.95 ± 4.66*	1.88 ± 0.06*△	3.19 ± 0.46*△
P			0.001	0.000	0.000

Table 2. Electrophysiological examination results of each group 5 week after modeling($\bar{x} \pm s$). OMST: Olmesartan. *P<0.05 vs. normal group, △P<0.05 vs. glucose injection model group.

Group	Time	Number of cases	SNCV(m/s)	*P*
C	One week	4	87.76 ± 6.16	0.626
	Five week	4	89.25 ± 6.36	
N-M	One week	4	76.96 ± 8.61	0.28
	Five week	4	69.48 ± 3.83	
U-M	One week	4	65.18 ± 2.82	0.02
	Five week	4	58.19 ± 3.58	

Table 3. SNCV examination results at 1 week and 5 weeks after modeling in the same group($\bar{x} \pm s$).

Statistical analysis

All statistical analyses were performed using SPSS 26.0. The results are expressed as the mean ± standard deviation ($\overline{X} \pm s$). Before analysis, the data were checked to determine whether they conformed to a normal distribution. Comparisons of two groups of independent samples that conformed to a normal distribution were performed using independent sample t tests. Comparisons of multiple groups of independent samples were performed using one-way ANOVA, and comparisons of nonnormally distributed data were performed using nonparametric tests. $P < 0.05$ indicated a statistically significant difference.

Results

Electrophysiological detection

Electrophysiological examination revealed significant differences in the amplitudes of the SNCV, DML and CMAP in each group 1 week after modeling. Pairwise comparison revealed differences between the ultrasound-guided injection model group and the other groups (Comparing the U-M group with the C group in SNCV, $P = 0.000$; Compared with the N-M group, $P = 0.045$. Comparing the U-M group with the C group in DML, $P = 0.000$; Compared with the N-M group, $P = 0.001$. Comparing the U-M group with the C group in CMAP, $P = 0.000$; Compared with the N-M group, $P = 0.000$.), but there were no differences between the other groups (Comparing the N-M group with the C group in SNCV, $P = 0.225$. Comparing the N-M group with the C group in DML, $P = 1.000$. Comparing the N-M group with the C group in CMAP, $P = 1.000$.). (Table 1)

Five weeks after modeling, the wave amplitudes of the SNCV, DML and CMAP in each group were significantly different. The differences in SNCV, DML and CMAP between the ultrasound-guided injection model group and the normal group were statistically significant ($P = 0.000$ in SNCV, $P = 0.000$ in DML, $P = 0.000$ in CAMP). There were significant differences in the DML and CMAP between the ultrasound-guided injection model group and the glucose injection model group ($P = 0.017$ in DML, $P = 0.000$ in CMAP), and there were significant differences in the CMAP between the normal group and the glucose injection model group ($P = 0.000$). The other differences were not statistically significant (Comparing the N-M group with the C group and U-M group in SNCV, $P = 0.065$. Comparing the C group with the N-M group in DML, $P = 0.605$). (Table 2)

Comparisons of the same group 1 week and 5 weeks after modeling, the CMAP of the glucose injection model group was significantly different ($P = 0.000$). The SNCV, DML and CMAP of the ultrasound-guided injection model group were significantly different ($P = 0.02$ in SNCV, $P = 0.001$ in DML, $P = 0.000$ in CAMP), but these parameters in the other groups were not significantly different (*Group C in SNCV*, $P = 0.626$; N-M group, $P = 0.28$. Group C in DML, $P = 0.589$; N-M group, $P = 0.053$. $P = 0.615$ in CMAP). (Tables 3, 4 and 5)

Group	Time	Number of cases	DML(ms)	t	*P*
C	One week	4	1.40 ± 0.14	-0.552	0.589
	Five week	4	1.44 ± 0.13		
N-M	One week	4	1.42 ± 0.16	-0.2114	0.053
	Five week	4	1.58 ± 0.14		
U-M	One week	4	1.72 ± 0.09		0.001
	Five week	4	1.96 ± 0.15		

Table 4. DML examination results at 1 week and 5 weeks after modeling in the same group($\bar{x} \pm s$). OMST: Olmesartan. **P*<0.05 vs. normal group, △*P*<0.05 vs. glucose injection model group.

Group	Time	Number of cases	CMAP amplitude(mv)	t	*P*
C	One week	4	7.49 ± 0.96	-0.514	0.615
	Five week	4	7.72 ± 0.83		
N-M	One week	4	7.36 ± 0.75	7.349	0.000
	Five week	4	4.17 ± 0.98		
U-M	One week	4	4.39 ± 1.28	4.787	0.000
	Five week	4	2.08 ± 0.44		

Table 5. CMAP amplitude examination results at 1 week and 5 weeks after modeling in the same group($\bar{x} \pm s$).

Group	Number of cases	median nerve diameter(mm)	TCL thickness(mm)
C	4	0.02 ± 0.0035	0.05 ± 0.0074
N-M	4	0.03 ± 0.0052	0.06 ± 0.0064
U-M	4	0.06 ± 0.0076*△	0.10 ± 0.013*△
P		0.000	0.000

Table 6. Ultrasonic test results of each group 1 week after modeling($\bar{x} \pm s$). OMST: Olmesartan. **P*<0.05 vs. normal group, △*P*<0.05 vs. glucose injection model group.

Group	Number of cases	median nerve diameter(mm)	TCL thickness(mm)
C	4	0.02 ± 0.0052	0.05 ± 0.0035
N-M	4	0.04 ± 0.0076	0.07 ± 0.0076
U-M	4	0.06 ± 0.0052*△	0.11 ± 0.0076*△
P		0.000	0.000

Table 7. Ultrasonic test results of each group 5 week after modeling($\bar{x} \pm s$). OMST: Olmesartan. **P*<0.05 vs. normal group, △*P*<0.05 vs. glucose injection model group.

Ultrasonic imaging detection

Ultrasound revealed that the median nerve diameter and TCL thickness of each group were significantly different 1 week and 5 weeks after modeling. Comparison between the two groups showed that the median nerve diameter and TCL thickness differed between the ultrasound-guided injection model group and the other groups (In the first week, median nerve diameter and U-M were compared with the C group, $P = 0.000$. The U-M group was compared with the N-M group, $P = 0.048$; Comparison of TCL thickness between U-M and C groups, $P = 0.000$; Compared with the N-M group, $P = 0.033$. In the fifth week, median nerve diameter and U-M were compared with the C group, $P = 0.000$. The U-M group was compared with the N-M group, $P = 0.048$; Comparison of TCL thickness between U-M and C groups, $P = 0.000$; Compared with the N-M group, $P = 0.048$.), but there were no differences between the other groups (In the first week, comparing median nerve diameter between group C and group N-M, $P = 0.098$; TCL diameter, compared between group C and N-M, $P = 0.178$. In the 5th week, comparing the median nerve diameter between group C and group N-M, $P = 0.111$; TCL diameter, compared between group C and N-M, $P = 0.098$.) (Tables 6 and 7).

One week and 5 weeks after modeling, the thickness of the TCL in the ultrasound-guided injection model group was significantly different ($P = 0.031$), but there were no significant differences in the other groups

Group	Time	Number of cases	median nerve diameter(mm)	*P*
C	One week	4	0.02 ± 0.0035	0.264
	Five week	4	0.02 ± 0.0052	
N-M	One week	4	0.03 ± 0.0052	0.084
	Five week	4	0.04 ± 0.0076	
U-M	One week	4	0.06 ± 0.0076	0.288
	Five week	4	0.06 ± 0.0052	

Table 8. Median nerve diameter inspection results at 1 week and 5 weeks after modeling in the same group($\bar{x} \pm s$).

Group	Time	Number of cases	TCL thickness(mm)	*P*
C组	One week	4	0.05 ± 0.007	0.09
	Five week	4	0.05 ± 0.0035	
N-M组	One week	4	0.06 ± 0.0064	0.102
	Five week	4	0.07 ± 0.0076	
U-M组	One week	4	0.10 ± 0.013	0.031
	Five week	4	0.11 ± 0.0076	

Table 9. TCL thickness inspection results at 1 week and 5 weeks after modeling in the same group($\bar{x} \pm s$).

(median nerve diameter, C group $P = 0.264$, N-M group $P = 0.084$, U-M group $P = 0.288$; TCL thickness, C group $P = 0.009$, N-M group $P = 0.102$) (Tables 8 and 9).

The ultrasonic images showed that the carpal tunnel in the same group did not change much 1 week or 5 weeks after modeling. The median nerve in the ultrasound-guided injection model group was significantly edematous and thickened, and the nerve in the glucose injection model group was slightly edematous, as shown by the red arrow. The transverse carpal ligament in the ultrasound-guided injection group was significantly thickened, but the change in the glucose injection model group was not obvious, as shown by the yellow arrow (Fig. 4).

Strain elastography (SE) revealed that the glucose injection model group and the ultrasound-guided injection model group exhibited increased tissue stiffness in the carpal tunnel compared to the normal group. However, the soft and hard changes in the glucose injection model group were not even. The hardness of the whole carpal tunnel in the ultrasound-guided injection model group obviously increased, beginning from the proximal boundary of the carpal tunnel, as shown by the red arrow. (Fig. 5)

H&E staining

H&E-stained sections showed that the collagen fibers in the normal group exhibited a tight and orderly arrangement, with uniform fiber spacing. The connections between nerve fibers and myelin sheaths were tight. (Fig. 6).

Compared to the normal group, the collagen fibers in the glucose injection model group were hyperplastic and loosely arranged, with slightly increased fiber gaps and slightly disordered tissue arrangement, as indicated by the yellow arrows. The difference was more obvious 5 weeks after model induction than at 1 week after model induction. The median nerve flattening rate decreased after 5 weeks of modeling.

Compared to the normal group and the glucose injection model group, the ultrasound-guided injection model group showed increased collagen fiber proliferation and significantly enlarged interstitial spaces, with more disordered collagen fiber bundles, as indicated by the yellow arrows. Neural edema was observed, with significant atrophy of nerve fibers and thinning of myelin sheaths, as indicated by the black arrows. The median nerve flattening rate was significantly reduced, with no significant differences between one week and five weeks after modeling.

TEM observation

Electron microscopy of the median nerve showed that the tissue structure of nerve fibers in the normal group was basically normal, the myelin sheath structure in myelinated nerve fibers was normal, and the fibers were arranged in a plate shape without fracture. The axons and myelin sheaths were closely arranged without vacuoles, and the cell bodies of Schwann cells were abundant and closely arranged.(Fig. 7).

Compared to the normal group, the nerve fiber tissue structure of the glucose injection model group was normal, and the myelin sheath was loose, but no structural damage occurred. There were gaps and vacuoles between axons and myelin sheaths, and these changes were more obvious 5 weeks after modeling than 1 week after modeling, as shown by the red arrow.

Compared to the normal group and the glucose injection model group, the nerve fiber tissue structure of the ultrasound-guided injection model group was abnormal, and the myelin sheath was loose. The myelin sheath was structurally damaged in some areas and broken and dissolved, as shown by the yellow arrow. There were

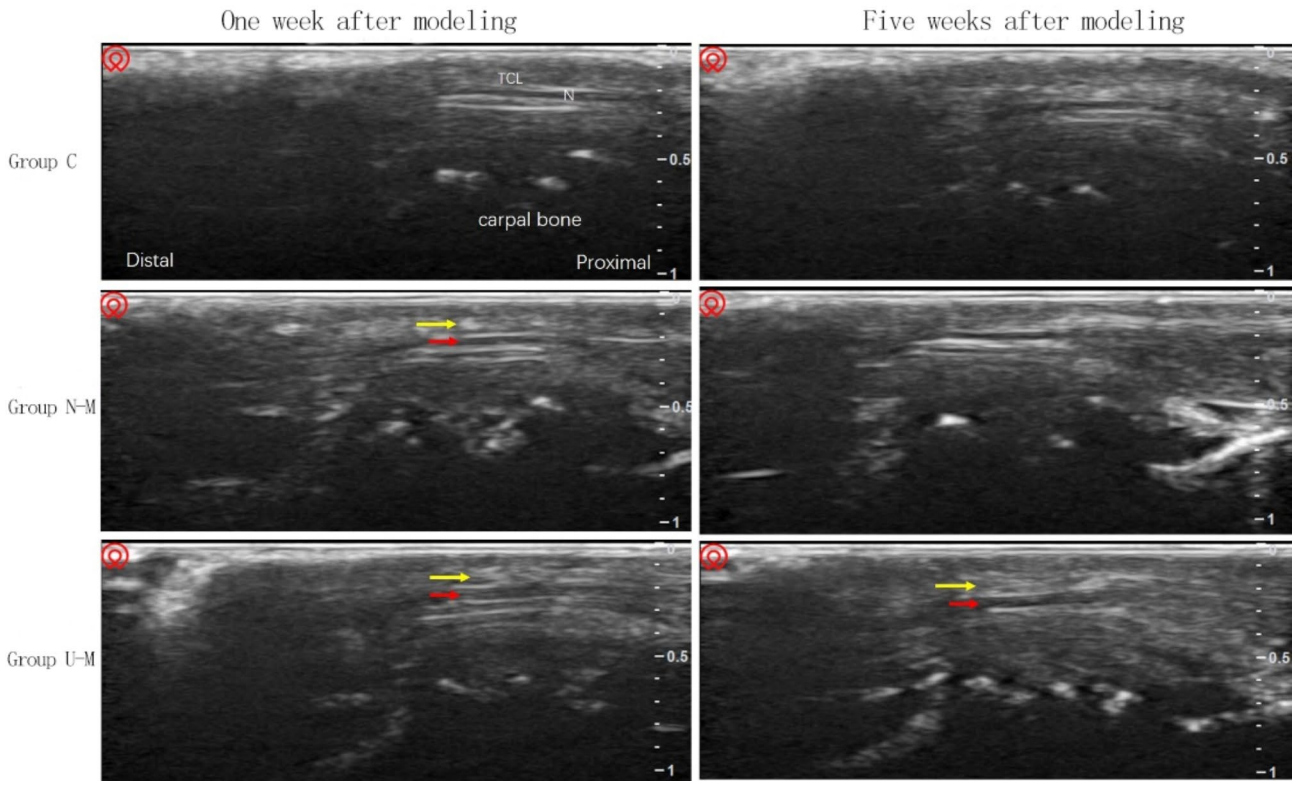

Fig. 4. Longitudinal ultrasonic sections of carpal tunnel in each group at 1 week and 5 weeks after modeling.

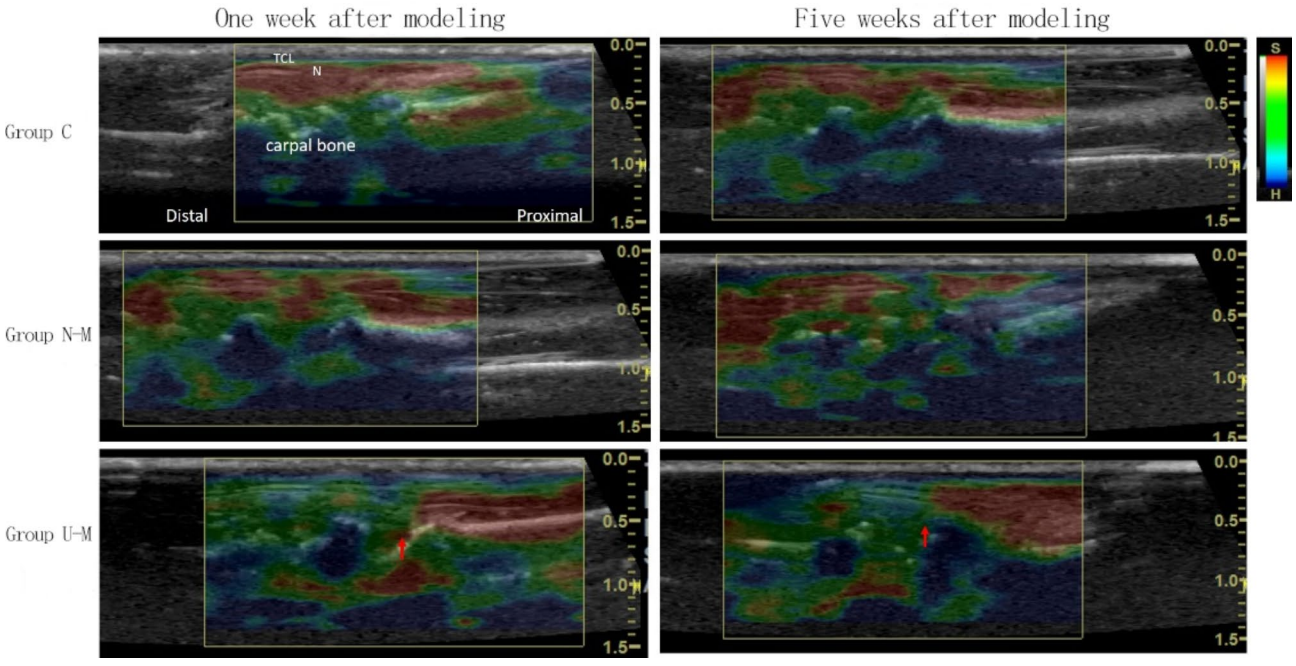

Fig. 5. Stress elastography of carpal tunnel in each group at 1 week and 5 weeks after modeling.

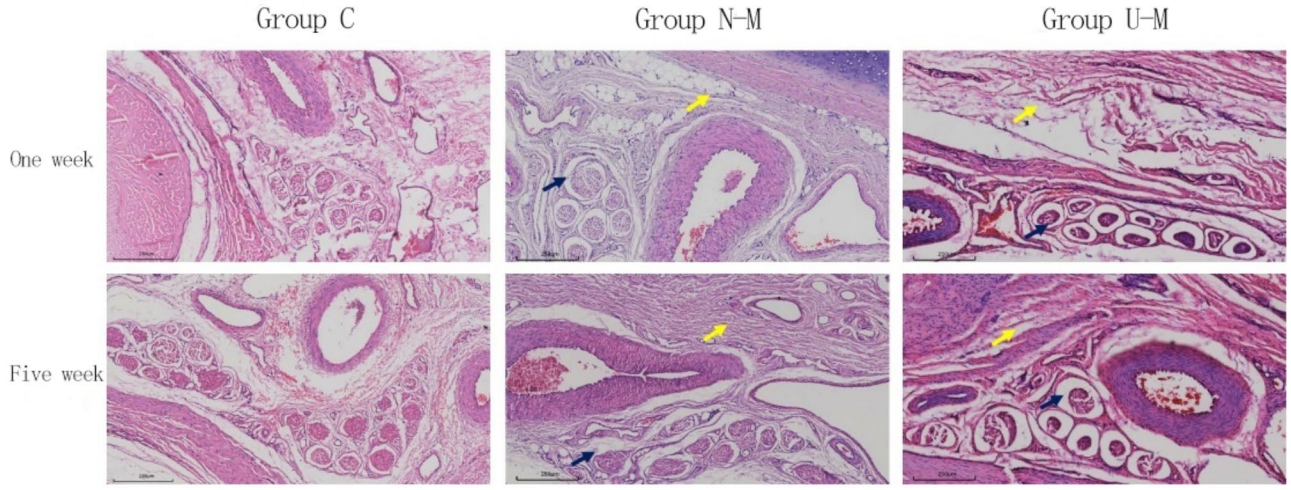

Fig. 6. Representative diagram of HE staining in each group at 1 week and 5 weeks after modeling.

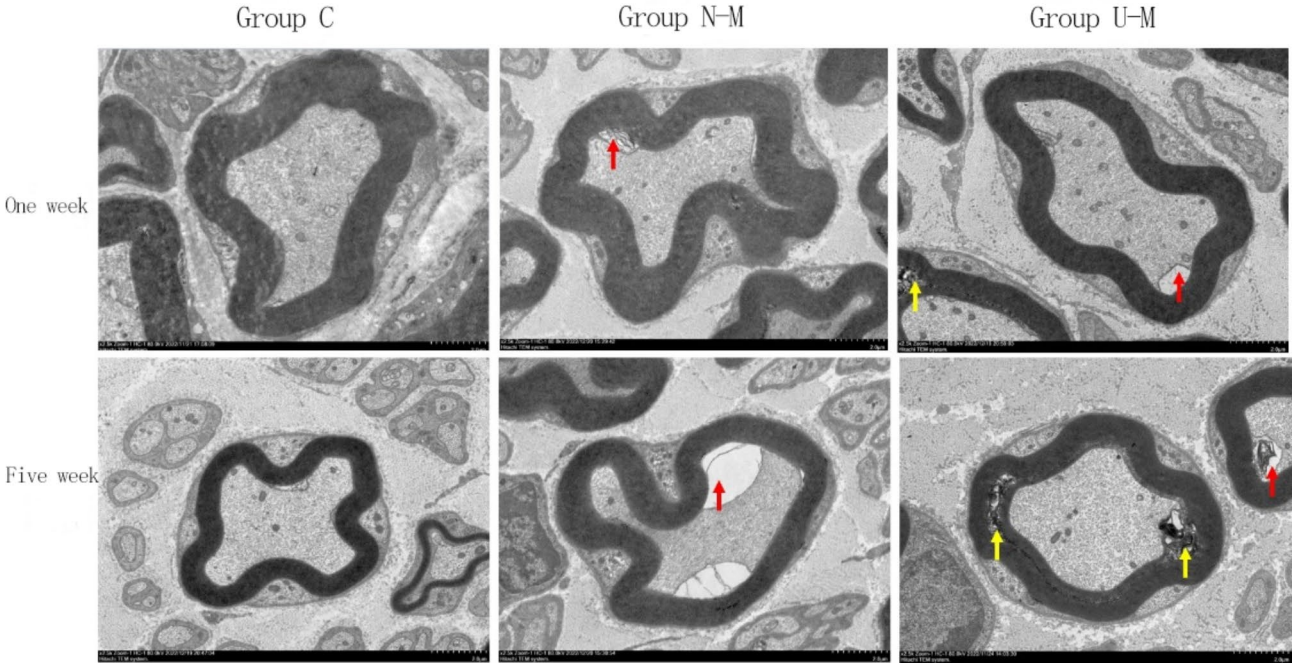

Fig. 7. Representative transmission electron micrographs of each group at 1 and 5 weeks after modeling.

gaps and vacuoles between axons and myelin sheaths, as shown by the red arrows. This difference was more obvious 5 weeks after modeling than 1 week after modeling.

Discussion

Selection of laboratory animal species

The choice of experimental animal species depends on the purpose of the research design. Study of the etiology and pathogenesis of CTS and evaluation of the efficacy of therapeutic methods are complex tasks. Therefore, to simulate the natural progression of human carpal tunnel syndrome as much as possible, experimental animals with physiological structures similar to the target population are needed. Some scholars[7] dissected the forepaws of rats, rabbits, dogs, and baboons and human upper limb specimens and examined the anatomical structure and SSCT of these animals using optical and scanning microscopy. They compared these findings with relevant human anatomical structures and ultrastructures. The anatomical structure and contents of the carpal tunnel in baboons and rabbits were similar to humans. However, the carpal tunnel in dogs does not contain superficial flexor tendons, and the carpal tunnel in rats is very small. The SSCT of human, baboon, and rabbit specimens

are very similar. Although baboons and rabbits are good animal models for studying the relationship between SSCT and CTS, rabbits are more practical.

The selection of experimental animals also requires physiological characteristics similar to humans. Modern research showed that carpal tunnel syndrome was also associated with increased pressure within the carpal tunnel, which requires a relatively rigid carpal tunnel[8]. The cause of increased pressure in the carpal tunnel is not known, and research on the etiology of carpal tunnel syndrome in humans is limited by the inability to longitudinally evaluate changes that occur before the onset of clinical symptoms. Animal models can overcome this limitation and provide opportunities to study the effects of gradually increasing carpal tunnel pressure on neural function and morphology. Therefore, appropriate animal models should have comparable anatomical structures and mechanical properties similar to human carpal tunnel.

Some scholars[9] measured the mechanical properties of carpal tunnels in a candidate animal model of carpal tunnel syndrome by measuring the resistance of a tapered metal rod passing through the carpal tunnel. The study used dogs, rabbits, rats, and freshly frozen human specimens. Comparison found that the human carpal tunnel was the longest and thickest, and the mouse carpal tunnel was the shortest and thinnest. The human carpal tunnel was also the stiffest, and the mouse carpal tunnel was the least stiff, with dogs and rabbits in the middle. The carpal tunnel in dogs exhibited the most similar mechanical properties to humans, followed by rabbits. This difference may be due to differences in the tissue properties of the transverse carpal ligament or the strength of the intercarpal ligament.

Considering its physiological and anatomical structure and biomechanical properties, the carpal tunnel of rabbits is most similar to humans, and the cost of purchasing and raising rabbits is relatively low[10]. Therefore, rabbits were selected as the experimental animals for the present study.

Selection of the rabbit carpal tunnel syndrome animal model

The pathogenesis of CTS is complex and inconclusive, and the modeling methods vary. Single-factor methods, such as glucose injection, surgical modeling, chemical induction, and pressure induction, are used to establish animal models of CTS in rabbits.

The injection of glucose solution is the simplest and easiest method to perform, but there is no uniform injection dose or frequency. Injection of hypertonic glucose induces local osmotic damage and triggers the release of growth factors and collagen deposition, which lead to the proliferation of connective tissue[11]. Some scholars[12–14] observed that one or two injections of 10% glucose induced subsynovial connective tissue fibrosis in a rabbit model, and two injections of higher concentrations of glucose had more significant effects than single injections. These studies revealed changes in the morphology, mechanical properties, and electrophysiology of the median nerve in the subsynovial connective tissue, but no neurological histological changes were observed. However, YOSHII[15] et al. demonstrated that higher doses produced more severe fibrosis, especially more severe neuropathy, and confirmed that this was a potentially useful animal model for studying the causes and treatment of CTS. This modeling method has strong reproducibility and a high success rate for large-scale animal experiments. It may also be used to investigate the effects and mechanisms of fibrosis on nerves and evaluate the efficacy of therapeutic methods. Due to the advantages of ultrasound, such as portability, lack of radiation, low cost, and high accuracy, its application in joint cavity injection has become increasingly common[2]. Similar animal studies confirmed that ultrasound guidance improved the accuracy of knee and temporomandibular joint injections in animal models, such as rabbits and rats[3–6]. Therefore, the present study used ultrasound-guided injection to improve the modeling method based on this model.

Some scholars[16] surgically removed the synovial connective tissue between the median nerve and the surface of the flexor digitorum tendon, sutured the transverse carpal ligament, and used adhesion to induce tissue damage and repair in the carpal tunnel. However, the surgery was complex, the model stability and success rate were low, and the model was not suitable for large-scale experiments. Another scholar[17–20] cut 5 mm of the superficial flexor tendon of the rabbit middle finger and sutured it together so that the surrounding subsynovial connective tissue was stretched and damaged. It is currently the only model simulating the effect of mechanics on the carpal tunnel and is suitable for studying CTS caused by damage and fibrosis of the subsynovial connective tissue due to shear stress. Due to the large amount of surgical trauma, complex surgery, and unknown long-term stability after modeling, further improvement of the surgical method is needed. The surgical modeling method also simulates carpal tunnel syndrome caused by increased pressure by reducing the volume of the carpal tunnel, but it is not recommended because the pressure cannot be quantified, and the modeling rate is unstable[21]. The pressure induction method involves the insertion of a No. 20 venous catheter into the carpal tunnel, with the catheter tip connected to a pressure sensor to monitor carpal tunnel pressure. Then, 36 °C sterile physiological saline is injected into the carpal tunnel to increase carpal tunnel pressure, which provides more precise control of pressure values and is similar to the pathogenesis of acute carpal tunnel syndrome in humans. It can be used for related studies of acute carpal tunnel syndrome within 2 weeks but not for studies lasting longer than 2 weeks[22–24]. Chemical induction does not cause any electrophysiological changes, but there are corresponding histopathological changes. This may be due to the short modeling cycle, during which neural dysfunction has not occurred, which requires further research and examination[25].

Comparison of the glucose injection method and improved ultrasound-guided modeling method

The present study evaluated the effect of four ultrasound-guided injections of 0.3 ml of a 10% glucose solution on rabbit carpal tunnel. Compared to previous modeling methods, we improved the injection method and dose. Previous studies[13,14] showed that injection without glucose did not cause any changes in nerve or SSCT, and the changes in rabbit carpal tunnel tissue were caused by glucose rather than injection trauma. Therefore, the present study did not use normal saline injection as the control group. A previous study[15] confirmed that multiple

injections of a 10% glucose solution had long-term effects on rabbit carpal tunnel tissue. These differences in electrophysiological parameters remained 8 to 12 weeks after modeling, but no short-term effects have been studied. Therefore, this study confirmed the short-term effect of multiple injections of a 10% glucose solution on rabbit carpal tunnel tissue, which was evaluated 1 week and 5 weeks after modeling.

Electrophysiological examination is one important criterion for evaluating carpal tunnel syndrome[26]. Clinically, the early pathophysiological changes in CTS are primarily demyelination and sensory fiber damage earlier than motor fiber damage. Therefore, SNCV abnormalities occur earlier than DML abnormalities. With disease progression, the DML increases, axonal damage occurs in the later stage, CMAP amplitude decreases, and atrophy occurs[27]. Therefore, the present study used the SNCV, DML and CMAP amplitudes as electrophysiological indicators to evaluate the success of the rabbit carpal tunnel syndrome model and the degree of median nerve lesion.

The electrophysiological results showed that the successful establishment of the ultrasound-guided injection model group took less time and was more stable. The amplitudes of the SNCV, DML and CMAP of the median nerve in the ultrasound-guided injection model group were significantly different from the normal group 1 and 5 weeks after modeling. The ultrasound-guided injection model group was successfully established 1 week after modeling, and the model remained stable in the disease state 5 weeks after modeling. However, the amplitudes of the SNCV, DML and CMAP of the median nerve in the glucose injection model group were not different from the normal group. Five weeks after modeling, the CMAP amplitude of the glucose injection model group was significantly different from the normal group, and the ultrasound-guided injection model group exhibited more obvious neurological dysfunction than the glucose injection model group. Therefore, the disease model in the glucose injection model group was not established 1 week after modeling. Only the CMAP amplitude was significantly different 5 weeks after modeling, and there was no difference in the SNCV or DML. Therefore, the model in this group was not fully established 5 weeks after modeling. Some studies observed significant DML prolongation only 12 weeks after modeling[15], which may be because the effect of glucose on carpal tunnel fibrosis is progressive. This observation is also consistent with the fact that CTS establishes a vicious circle of disease development without intervention. The differences within the same group 1 week and 5 weeks after modeling also supports this characteristic.

The injection volume of 0.1 ml in the original modeling method[15] is too small. The lack of ultrasound guidance prevents the accurate spreading of the glucose solution around the median nerve, which prevents the rapid development and establishment of the model. The improved modeling method in the present study is different from the original modeling method. First, ultrasound was introduced to perform ultrasound-guided injection and achieve an accurate injection. Second, the injection dose was increased. Pre-experiments showed that a dose of 0.1 ml only contacted part of the median nerve. When the dose was increased to 0.3 ml, the glucose solution wrapped the entire median nerve and filled the carpal tunnel (Fig. 2). Ultrasound guided the injection in real time and allowed evaluation of the severity of carpal tunnel syndrome. With the development of ultrasound technology, ultrasound imaging has been proven to be another key technology for evaluating carpal tunnel tissue[28] and may be used to diagnose carpal tunnel lesions and evaluate the prognosis of disease treatment[29–31]. In addition to two-dimensional ultrasound detection, ultrasonic elastography (UE) technology has recently been developed to visually, qualitatively and quantitatively detect the mechanical properties of various tissues using ultrasound, and it may be used to evaluate the elasticity of various tissues[32]. Studies[33,34] have shown that ultrasonic elastography combined with two-dimensional ultrasound may be used to diagnose carpal tunnel syndrome.

Therefore, the present study used two-dimensional ultrasound and ultrasonic elastography to detect and evaluate changes in carpal tunnel tissue morphology and mechanical properties. Two-dimensional ultrasound images showed that the transverse carpal ligament was thickened, and the median nerve was significantly edematous in the ultrasound-guided injection model group after modeling. These changes were significantly different from the normal group, and the thickness of the TCL was significantly greater 5 weeks after modeling compared to 1 week after modeling. However, the changes in the glucose injection model groups were smaller, and there was no significant difference between the two groups. Ultrasound examination found that four injections of 0.3 ml of a 10% glucose solution under ultrasound guidance caused SSCT fibrosis and thickening of the transverse carpal ligament. This finding is consistent with the hypothesis of the etiology of carpal tunnel syndrome, i.e., the increased pressure in the carpal tunnel caused by thickening of the transverse carpal ligament is one of the main causes of carpal tunnel syndrome[35].

Stress elastography revealed that the carpal tunnel was red and green in the glucose injection model group, which indicated uneven changes in tissue fibrosis. The color changed from the proximal boundary of the carpal tunnel to blue–green in the ultrasound-guided injection model group, which indicated that the tissue fibrosis in the whole carpal tunnel became rigid from the proximal carpal tunnel. These results are consistent with the injection site under our ultrasound guidance, which highlights the accuracy of ultrasound guidance.

Histopathological examination of the carpal tunnel and median nerve in the ultrasound-guided injection model group also confirmed the electrophysiology and ultrasound imaging results. According to the results of H&E staining and transmission electron microscopy, the median nerve showed obvious atrophy of nerve fibers, a thin myelin sheath, a reduced flattening rate and axonal injury, increased proliferation of collagen fibers, a significantly enlarged gap, and more scattered collagen fiber bundles.

However, the H&E staining and transmission electron microscopy results showed that the median nerve in the glucose injection model group was demyelinated, and no obvious axonal injury was observed. However, the electrophysiological results showed that the amplitude of the CMAP was significantly reduced. This finding contradicts the electrophysiological changes in patients with clinical CTS. The following reasons for these findings are offered: ① the sample size may have been too small and resulted in no changes in the SNCV or DML being detected; and ② the nerve axon injury section may not have been cut when the morphological tissue

sections were made. This finding also confirmed the stability of the ultrasound-guided injection model group from another perspective.

Conclusion

Electrophysiological, ultrasound imaging and histomorphological detection revealed that four injections of 0.3 ml of a 10% glucose solution under ultrasound guidance aggravated fibrosis and significantly altered the nerve histology of the TCL and SSCT in the rabbit carpal tunnel and led to significant neurological dysfunction. Compared to the original modeling method, this modeling method reduced the time required for successful establishment of the disease model and exhibited high stability after modeling. This technique is a simple and feasible method for establishing a rabbit carpal tunnel syndrome model.

Data availability

The datasets generated during and/or analysed during the current study are available from the corresponding author and the first author on reasonable request.

Received: 27 September 2024; Accepted: 6 March 2025
Published online: 10 March 2025

References

1. Sevy, J. O., Sina, R. E. & Varacallo, M. Carpal tunnel syndrome. In: StatPearls. Treasure Island (FL): StatPearls Publishing; October 29, (2023).
2. Bodor, M., Murthy, N. & Uribe, Y. Ultrasound-guided cervical facet joint injections. *Spine J.* **22** (6), 983–992 (2022).
3. Ruiz, A. et al. Accuracy of ultrasound-guided versus landmark-guided intra-articular injection for rat knee joints. *Ultrasound. Med. Biol.* **45** (10), 2787–2796 (2019).
4. Wang, Y. et al. Accuracy and feasibility of Ultrasound-Guided Intra-articular injection of the rat hip joint. *Ultrasound Med. Biol.* **47** (10), 2936–2940 (2021).
5. Norvall, A., Cota, J. G., Pusterla, N. & Cissell, D. Ultrasound-guided arthrocentesis of the temporomandibular joint in healthy adult horses is equivalent to blind arthrocentesis. *Vet. Radiol. Ultrasound.* **61** (3), 346–352 (2020).
6. Jarosinski, S. K., Sampson, S. N. & Russell, L. Ultrasound-assisted injection of the centrodistal joint in the horse. *Equine Vet. J.* **53** (4), 817–825 (2021).
7. Ettema, A. M. et al. Comparative anatomy of the subsynovial connective tissue in the carpal tunnel of the rat, rabbit, dog, baboon, and human. *Hand* **1** (2), 78–84 (2006).
8. Joshi, A. et al. Carpal tunnel syndrome: pathophysiology and comprehensive guidelines for clinical evaluation and treatment. *Cureus*, **14**(7). (2022).
9. Tung, W. L. et al. Comparative study of carpal tunnel compliance in the human, dog, rabbit, and rat. *J. Orthop. Res.* **28** (5), 652–656 (2010).
10. Hou, Y. et al. Genetically modified rabbit models for cardiovascular medicine. *Eur. J. Pharmacol.* **922**, 174890 (2022).
11. Waluyo, Y., Artika, S. R., Wahyuni, I. N., Gunawan, A. M. A. K. & Zainal, A. T. F. Efficacy of prolotherapy for osteoarthritis: A systematic review. *J. Rehabil Med.* **55**, jrm00372 (2023). Published 2023 Feb 27.
12. Oh, S. et al. Dextrose-induced subsynovial connective tissue fibrosis in the rabbit carpal tunnel: a potential model to study carpal tunnel syndrome? *Hand* **3** (1), 34–40 (2008).
13. Yoshii, Y. et al. The effects of hypertonic dextrose injection on connective tissue and nerve conduction through the rabbit carpal tunnel. *Arch. Phys. Med. Rehabil.* **90** (2), 333–339 (2009).
14. Yoshii, Y. et al. Effects of hypertonic dextrose injections in the rabbit carpal tunnel. *J. Orthop. Res.* **29** (7), 1022–1027 (2011).
15. Yoshii, Y. et al. Effects of multiple injections of hypertonic dextrose in the rabbit carpal tunnel: a potential model of carpal tunnel syndrome development. *Hand* **9** (1), 52–57 (2014).
16. Hachinota, A. et al. Preventive effect of alginate gel formulation on perineural adhesion. *J. Hand Surg. (Asian-Pacific Volume)*. **25** (02), 164–171 (2020).
17. Moriya, T. et al. Tendon injury produces changes in SSCT and nerve physiology similar to carpal tunnel syndrome in an in vivo rabbit model. *Hand* **6** (4), 399–407 (2011).
18. Sun, Y. L. et al. Subsynovial connective tissue is sensitive to surgical interventions in a rabbit model of carpal tunnel syndrome. *J. Orthop. Res.* **30** (4), 649–654 (2012).
19. Vanhees, M. et al. The effect of time after shear injury on the subsynovial connective tissue and median nerve within the rabbit carpal tunnel. *Hand* **8** (1), 54–59 (2013).
20. Chikenji, T. et al. Transforming growth factor-β (TGF-β) expression is increased in the subsynovial connective tissue in a rabbit model of carpal tunnel syndrome. *PloS One*. **9** (9), e108312 (2014).
21. Lluch, A. L. Thickening of the synovium of the digital flexor tendons: cause or consequence of the carpal tunnel syndrome? *J. Hand Surg.* **17** (2), 209–211 (1992).
22. Paik, N. J., Cho, S. H. & Han, T. R. Ultrasound therapy facilitates the recovery of acute pressure-induced conduction block of the median nerve in rabbits. *Muscle Nerve*. **26** (3), 356–361 (2002).
23. Diao, E. et al. Carpal tunnel pressure alters median nerve function in a dose-dependent manner: a rabbit model for carpal tunnel syndrome. *J. Orthop. Res.* **23** (1), 218–223 (2005).
24. Lim, J. Y. et al. Dose-responsiveness of electrophysiologic change in a new model of acute carpal tunnel syndrome. *Clin. Orthop. Relat. Research®*. **427**, 120–126 (2004).
25. Rosen, H. R. et al. Chemically-induced chronic nerve compression in rabbits–a new experimental model for the carpal tunnel syndrome. *Langenbecks Arch. Chir.* **377** (4), 216–221 (1992).
26. Jablecki, C. K. et al. Practice parameter: electrodiagnostic studies in carpal tunnel syndrome. *Neurology* **58** (11), 1589–1592 (2002).
27. Shen, S. H. et al. A comparative study of median neuropathy in carpal tunnel syndrome between multimodal ultrasound and nerve electrophysiological testing. *Chin. J. Ultrasound Med.* **39** (06), 688–692 (2023).
28. Padua, L. et al. Carpal tunnel syndrome: updated evidence and new questions. *Lancet Neurol.* **22** (3), 255–267 (2023).
29. Levy, M. et al. Technique for ultrasound-guided intraarticular cervical articular process injection in the dog. *Vet. Radiol. Ultrasound*. **55** (4), 435–440 (2014).
30. Osiak, K., Elnazir, P., Walocha, J. A. & Pasternak, A. Carpal tunnel syndrome: state-of-the-art review. *Folia Morphol. (Warsz)*. **81** (4), 851–862 (2022).
31. Lam, K. H. S. et al. Ultrasound-Guided interventions for carpal tunnel syndrome: A systematic review and Meta-Analyses. *Diagnostics (Basel)*. **13** (6), 1138 (2023). Published 2023 Mar 16.

32. Nakamura, M. & Akagi, R. Ultrasonic shear-wave elastography: A novel method for assessing musculoskeletal soft tissue and nerves. *Clin. Neurophysiol.* **140**, 163–164 (2022).
33. Nam, K. et al. Diagnosis of carpal tunnel syndrome using shear wave elastography and high-frequency ultrasound imaging. *Acad. Radiol.* **28** (9), e278–e287 (2021).
34. Asadov, R. et al. The effectiveness of ultrasonography and ultrasonographic elastography in the diagnosis of carpal tunnel syndrome and evaluation of treatment response after steroid injection. *Eur. J. Radiol.* **108**, 172–176 (2018).
35. He, W. H. et al. The clinical application of the theory of master tendons controlling bones and facilitating organs in meridian tendon diseases. *Hunan J. Traditional Chin. Med.* **35** (5), 155–157 (2019).

Author contributions
Q.Y. made the conception and design of the study, Q.Y. and T.H. made manuscript drafting and critical revision, J.Y. and D.T. made data analysis, Y.N. and Q. made acquisition of data, S.L. made approval of final version of manuscript.

Funding
National Natural Science Foundation (Youth Science Foundation Project) (No.82104886); Natural Science Foundation of Fujian Province (No.2021J01932); NATCM's Project of High-level Construction of Key TCM Disciplines (Traditional Chinese Orthopedics)(Grant number: zyyzdxk-2023106); Traditional Chinese Orthopedics Open subject of FJTCM (Grant number: XGS2023019).

Declarations

Competing interests
The authors declare no competing interests.

Additional information
Correspondence and requests for materials should be addressed to S.-L.L.

Reprints and permissions information is available at www.nature.com/reprints.

Publisher's note Springer Nature remains neutral with regard to jurisdictional claims in published maps and institutional affiliations.